Reduced Graphene Oxide Intercalated MgAl-Layered Double Hydroxide for Photocatalytic Degradation of Various Organic Dyes under Ultraviolet and Visible Light Illumination

Halah Arishi , Ghalia Alzahrani , Mohamed Mokhtar M Mostafa *

Posted Date: 20 October 2025

doi: 10.20944/preprints202510.1526.v1

Keywords: nanocomposite; photocatalysis; metal oxide; degradation; reduced graphene oxide

Article

Reduced Graphene Oxide Intercalated MgAl-Layered Double Hydroxide for Photocatalytic Degradation of Various Organic Dyes under Ultraviolet and Visible Light Illumination

Halah Arishi [1,2], Ghalia Alzhrani [1] and Mohamed Mokhtar [1,3,*]

[1] Chemistry Department King Abdulaziz University,21589 Jeddah, P.O. Box 80203, Saudi Arabia

[2] Department of Physical Sciences; Jazan University; P.O. Box.114, Jazan 45142, Saudi Arabia

[3] Center of Excellence for Advanced Materials Research (CEAMR); King Abdulaziz University; Jeddah 21589, Saudi Arabia

* Correspondence: mmoustafa@kau.edu.sa; Tel.: +966-500558045; Fax: +966-2-6952292

Abstract

This study reports the fabrication of a novel series of photocatalysts based on reduced graphene oxide (rGO) intercalated into magnesium aluminum layered double hydroxides (MgAl-LDH), denoted as LDH/rGO(0.25), LDH/rGO(0.5), and LDH/rGO(0.75), where the numeric values represent the mass ratio of LDH to rGO. These nanocomposites were designed to address the escalating issue of organic dye pollution in wastewater. The incorporation of rGO into the LDH matrix significantly improved the electrical conductivity, surface area, and light-harvesting capacity of the hybrid material. Importantly, rGO intercalation led to a notable narrowing of the optical band gap of pristine MgAl-LDH (initially 3.5 eV) to values ranging from 2.4 to 2.9 eV, depending on the rGO content. This reduction enhanced the absorption of visible light and promoted more efficient charge carrier separation and migration. The structural, morphological, and optical properties of the synthesized composites were systematically investigated using FTIR, TEM, and UV–Vis's spectroscopy. The photocatalytic performance was evaluated under both ultraviolet (UV) and visible light irradiation, focusing exclusively on the degradation of the Malachite Green (MG) dye as a representative organic pollutant. Among the composites, LDH/rGO(0.25) exhibited the highest degradation efficiency, achieving up to 93% removal of MG within 50 minutes under optimal conditions (pH=10, dye concentration of 10 ppm, and appropriate catalyst dosage). The improvement of photocatalytic activity is assigned to the synergistic interaction between the LDH layers and rGO nanosheets, as well as the optimized band structure induced by varying rGO content. These findings demonstrate the promising potential of LDH/rGO nanohybrids particularly LDH/rGO (0.25) and LDH/rGO (0.5) as efficient, visible-light-responsive photocatalysts for sustainable wastewater treatment applications.

Keywords: nanocomposite; photocatalysis; metal oxide; degradation; reduced graphene oxide

1. Introduction

Water contamination by synthetic dyes has become an urgent global challenge due to their high toxicity, chemical stability, and resistance to biodegradation. These pollutants commonly derived from textile, printing, and pharmaceutical industries persist in aquatic systems and pose severe ecological and health risks, including mutagenicity and carcinogenicity [1,2]. The complex aromatic structures and strong chromophoric bonds of dyes such as malachite green (MG), methyl orange (MO), and crystal violet (CV) hinder their natural decomposition, necessitating the development of advanced and sustainable remediation technologies [3]. Among the available methods,

 doi:10.20944/preprints202510.1526.v1

photocatalytic degradation has emerged as a highly promising approach for wastewater purification. Unlike conventional treatments (e.g., adsorption, coagulation, or oxidation), photocatalysis directly decomposes organic pollutants into harmless by-products such as CO_2 and H_2O through redox reactions initiated by light irradiation [4]. This process offers multiple advantages low energy demand, environmental compatibility, reusability of catalysts, and the absence of secondary pollution—making it a green alternative for large-scale water treatment [5,6]. In recent years, Layered Double Hydroxides (LDHs) have gained considerable attention as efficient semiconductor photocatalysts due to their highly ordered brucite-like layers, adjustable metal cation composition, and interlayer anion-exchange capacity [7]. These structural features enable the tuning of electronic and surface properties, which directly influence charge transfer and pollutant adsorption during photocatalysis. Among LDHs, magnesium–aluminum variants (MgAl-LDHs) have been extensively studied for dye degradation because of their excellent chemical stability, abundance, and capability to form hybrid nanocomposites with functional materials [8]. However, pristine MgAl-LDHs suffer from intrinsic limitations such as a wide band gap (≈3.0–3.2 eV), rapid recombination of photogenerated electron–hole pairs, and weak visible-light response—that significantly restrict their catalytic efficiency [9–11].

These challenges have led researchers to explore composite systems where LDHs are coupled with conductive carbonaceous materials such as graphene oxide (GO) or reduced graphene oxide (rGO), thereby forming highly synergistic heterostructures [9]. Reduced graphene oxide (rGO), a two-dimensional sp^2-hybridized carbon nanomaterial, provides outstanding electronic conductivity, high surface area, and a π-conjugated network that facilitates rapid electron mobility [12]. When integrated with LDHs, rGO functions as an electron sink—accepting photogenerated electrons from the LDH conduction band—thus suppressing charge recombination and extending the carrier lifetime [13,14]. This electron mediation enhances the generation of reactive oxygen species (ROS), such as hydroxyl (•OH) and superoxide ($\bullet O_2^-$) radicals, which play a pivotal role in oxidative dye degradation [15]. Furthermore, the π–π interactions between the aromatic rings of dyes and the conjugated structure of rGO promote efficient adsorption, providing intimate contact between the dye molecules and active catalytic sites. MgAl-LDH and its modified composites have been extensively studied for the photocatalytic degradation of methyl orange (MO) under various light irradiation conditions. While pristine MgAl-LDH exhibits moderate photocatalytic performance, its activity can be significantly enhanced through compositing with semiconducting materials such as TiO_2, g-C_3N_4, and graphene-based derivatives. These modifications improve light absorption capacity and facilitate more efficient separation of photogenerated electron–hole pairs, thereby enhancing overall photocatalytic efficiency. Photodegradation of MO using MgAl-LDH-based photocatalysts typically follows pseudo-first-order kinetics. The degradation efficiency is strongly influenced by the physicochemical properties of the LDH, including the nature of interlayer anions, surface area, band gap, pH of the solution, and the type of light source. Optimized composites have demonstrated remarkable removal efficiencies exceeding 90% within short irradiation periods, primarily due to the generation of reactive oxygen species such as hydroxyl (•OH) and superoxide ($\bullet O_2^-$) radicals. These findings underscore the potential of MgAl-LDH-based photocatalysts as effective materials for the treatment of dye-contaminated wastewater [14]. On the other hand, the photocatalytic degradation of Malachite Green (MG), a toxic cationic dye, was systematically investigated using reduced graphene oxide–zirconia (rGO-ZrO_2) nanocomposites under visible light irradiation. Among the synthesized materials, the nanocomposite containing 5 wt% rGO (denoted as ZG5MR) exhibited the highest photocatalytic performance, achieving a degradation efficiency of 98.2% within 100 minutes. The enhanced photocatalytic activity of ZG5MR is primarily attributed to its reduced band gap energy (2.90 eV), which enables effective visible light absorption, and its high specific surface area (86 m^2/g), providing abundant active sites for dye adsorption and reaction [15].

Given these insights, the present work aims to systematically investigate the photocatalytic efficiency of MgAl–LDH/rGO nanocomposites toward the degradation of Malachite Green (MG) dye. The study seeks to elucidate the role of molecular structure and electronic interactions between the

 doi:10.20944/preprints202510.1526.v1

catalyst and the MG chromophore in governing the degradation mechanism. Understanding this relationship is essential for the rational design of next generation photocatalysts for organic pollutant removal.

2. Results and Discussion

2.1. Physicochemical and Structural Characterization

Detailed physicochemical and structural characterization results including XRD, FTIR, BET, and TEM analyses, are provided in the Supplementary Materials (Section S1, Figures S1–S4 and Table S1).

2.2. Optical Properties

In Figure 1 was an analysis of UV-Vis Absorbance data. The diffuse reflectance spectra of the samples (MgAl-LDH, GO, rGO, and LDH/rGO composites) reveal the absorbance properties of the materials across the UV and visible wavelength ranges. MgAl-LDH exhibits absorbance mainly in the UV range, corresponding to its wide bandgap semiconductor behavior. GO and rGO absorbance shifts toward the visible region due to the introduction of $\pi \rightarrow \pi^*$ transitions from conjugated carbon networks and the reduction of oxygen functionalities in rGO [16,17]. Figure 1. LDH/rGO composites show intermediate behavior, where increasing rGO content (e.g., LDH/rGO 0.25 to 0.75) results in a noticeable redshift, enhancing absorption in the visible spectrum.

In Figure 2 reflectance decreases significantly for composites with higher rGO content, reflecting better light absorption properties due to the incorporation of reduced graphene oxide. MgAl-LDH shows the highest reflectance, while rGO exhibits the lowest. The bandgap (Eg) values were calculated using the Kubelka-Munk function and Tauc plot for indirect bandgap materials (Figure 3). The following trends were observed: MgAl-LDH: 3.5 eV (wide bandgap, UV active). GO: 3.5 eV (similar to LDH due to its oxidized structure). rGO: 2.3 eV (narrowed due to restored conjugated structure). LDH/rGO Composites: LDH/rGO (0.25): 2.4 eV, LDH/rGO (0.5): 2.8 eV, and LDH/rGO (0.75): 2.9 eV in Table 1. The narrowing bandgap with increasing rGO content reflects the improved ability to absorb visible light, which is essential for photocatalytic applications. The composites exhibit enhanced visible-light activity, which is directly correlated to the introduction of rGO and the narrowing of the bandgap. The interaction between MgAl-LDH and rGO in the composites leads to better light-harvesting capabilities, making them suitable candidates for photocatalytic or light-assisted degradation processes [18]. Optimization of LDH/rGO (0.5) shows an optimal balance between light absorption and bandgap energy, making it a promising material for further studies. Finally, the UV-DRS analysis demonstrates that the integration of rGO into the MgAl-LDH structure significantly enhances the optical properties by reducing the bandgap and improving visible-light absorption. These findings validate the composites' potential for photocatalytic applications, such as degradation of pollutants or solar energy harvesting.

 doi:10.20944/preprints202510.1526.v1

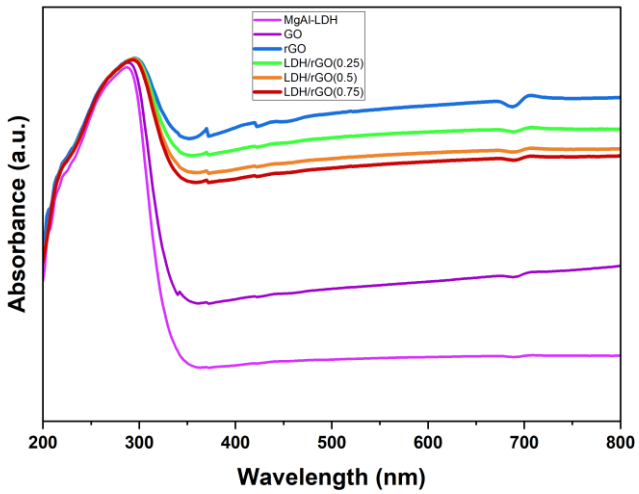

Figure 1. UV–Vis Absorption Spectra of MgAl-LDH, GO, rGO, and LDH/rGO Composites.

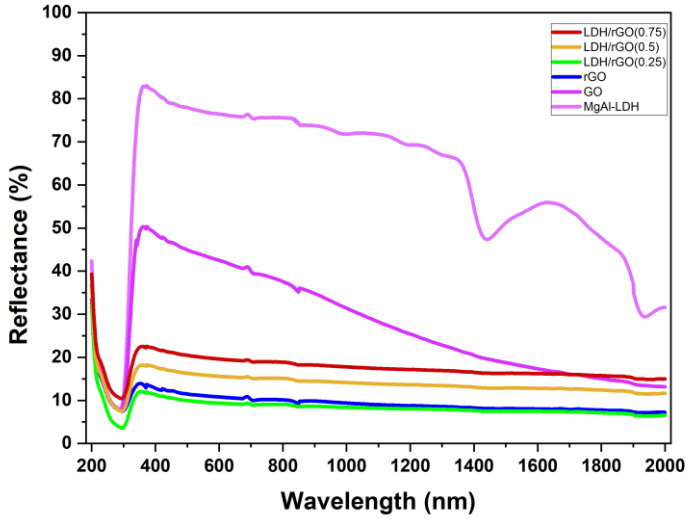

Figure 2. Diffuse Reflectance Spectra (DRS), of MgAl-LDH, GO, rGO, and LDH/rGO Composites.

 doi:10.20944/preprints202510.1526.v1

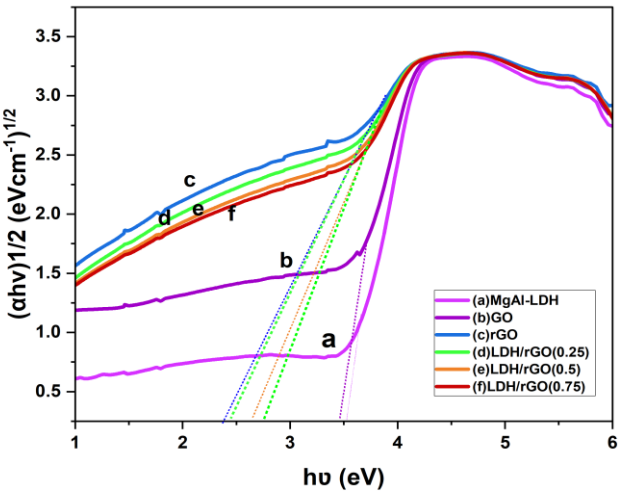

Figure 3. Tauc Plot for Band Gap Estimation of MgAl-LDH, GO, rGO, and LDH/rGO Composites.

Table 1. Comparison of the band gap values of the prepared samples.

N#	Samples	Band Gap, Eg [eV] for the Prepared Samples
a	MgAl-LDH	3.5eV
b	GO	3.5eV
c	rGO	2.3eV
d	LDH/rGO[0.25]	2.4eV
e	LDH/rGO[0.5]	2.8eV
f	LDH/rGO[0.75]	2.9eV

Figure 4 displays PL intensity across a range of wavelengths, highlighting the emission characteristics of each material. Variations in intensity and peak positions can indicate differences in electronic structures and interactions within the materials [19]. MgAl-LDH exhibits specific emission peaks, reflecting its inherent electronic properties. Graphene Oxide (GO) displays higher PL intensity compared to MgAl-LDH, attributed to defects and oxygen-containing functional groups that enhance recombination of electron-hole pairs. Reduced Graphene Oxide (rGO) shows reduced PL intensity compared to GO, indicating fewer oxygen groups and a decrease in electron-hole recombination due to better conductivity. Composites of LDH/rGO with varying rGO content (0.25, 0.5, and 0.75) likely exhibit PL intensities that correlate with the amount of rGO incorporated, influencing the overall emission characteristics. A trend of varying PL intensities is observed as the rGO content increases. The composite with 0.75 weight percentage rGO likely has the lowest PL intensity (LDH/rGO(0.25)), suggesting enhanced charge separation and suppression of electron-hole recombination. This trend indicates that integrating rGO into the LDH structure improves charge transport properties and reduces recombination, which is crucial for photocatalytic and optoelectronic applications.

 doi:10.20944/preprints202510.1526.v1

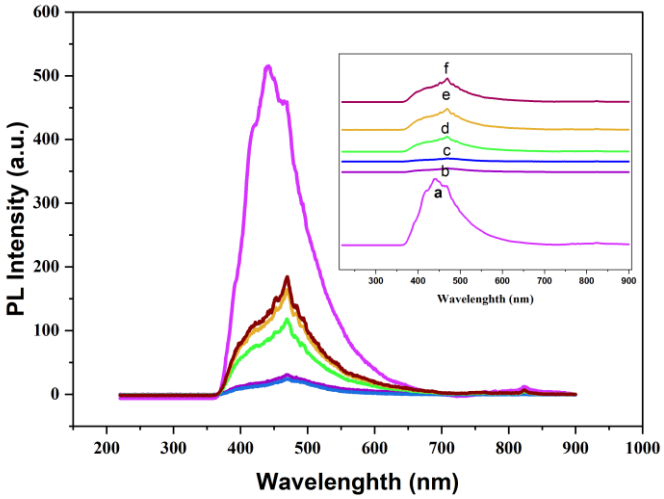

Figure 4. Photoluminescence [PL] spectra of [a] MgAl-LDH, [b] GO, [c] rGO, and LDH/rGO composites with varying rGO content [d]0.25, [e]0.5, and [f] 0.75].

2.3. Electrochemical Analysis

To enhance the understanding of the electrical charge transport kinetics in the heterostructure material, Electrochemical Impedance Spectroscopy (EIS) measurements were conducted to elucidate the charge transfer resistance (Rct) at the electrode/electrolyte interface. The diameter of the arc radius in the semicircle within the high-frequency region of the electrode material serves as an indicator of the charge transfer resistance (Rct) across the electrode/electrolyte interface [20,21].

Electrochemical impedance spectroscopy (EIS) results are presented in the form of Bode plots for both phase angle and impedance magnitude [20]. The comparative Bode phase plot shown in Figure 5a offers valuable insights into the frequency-dependent electrochemical behavior of the samples of pristine MgAl-LDH, reduced graphene oxide (rGO), and their hybrid composites at different ratios LDH/rGO(0.25), LDH/rGO(0.5), and LDH/rGO(0.75). The phase angle variation across the frequency spectrum reflects the interplay between resistive and capacitive properties and highlights the impact of composition on the interfacial dynamics and charge transport efficiency. At low frequencies (1–10 Hz), all samples exhibit relatively low phase angles, indicating significant charge transfer resistance and limited capacitive response. Among them, MgAl-LDH shows the lowest initial phase angle (~5°), confirming its poor electronic conductivity and sluggish ion transport. Conversely, rGO and LDH/rGO composites demonstrate improved low-frequency responses, with LDH/rGO(0.75) achieving the highest phase value (~18°), suggesting enhanced interfacial polarization and lower resistance due to the synergistic effect of conductive rGO and electroactive LDH domains. In the intermediate frequency range (~10^2–10^3 Hz), distinct differences emerge in the peak phase angles. LDH/rGO(0.25) shows the highest maximum (~60°), reflecting optimal capacitive performance due to an effective balance between rGO conductivity and LDH redox activity. LDH/rGO(0.75) also exhibits a high phase angle (~59°), indicating strong pseudocapacitive behavior, though the broader peak may suggest slower relaxation dynamics and increased structural heterogeneity. LDH/rGO(0.5) and rGO show moderate maxima (~50–52°), while MgAl-LDH remains the lowest, consistent with its minimal contribution to capacitive storage. At high frequencies (>10^3 Hz), all samples display a downward trend in phase angle, transitioning to resistive behavior as double-layer formation becomes ineffective at rapid perturbation rates. The rate and degree of this decline offer further contrast: rGO and LDH/rGO(0.25) retain higher phase values over a broader range, reflecting better frequency response and faster polarization-depolarization kinetics. In contrast, MgAl-LDH and LDH/rGO(0.75) exhibit more pronounced drops, implying

 doi:10.20944/preprints202510.1526.v1

lower responsiveness under dynamic conditions. Taken together, the analysis reveals that LDH/rGO(0.25) outperforms other compositions in terms of both maximum phase angle and retention across frequencies, suggesting superior charge separation, interfacial capacitance, and electronic pathways. The observed trend highlights the importance of compositional tuning in LDH-based hybrids: Excessive LDH content (as in LDH/rGO(0.75)) may introduce diffusion limitations and hinder conductivity. Insufficient LDH content (pure rGO) may lack sufficient electroactive sites for pseudocapacitive storage. Intermediate composition (LDH/rGO(0.25)) appears to offer the most favorable electrochemical performance.

Figure 5b displays the Bode impedance (|Z|) plot for pristine MgAl-LDH, reduced graphene oxide (rGO), and a series of LDH/rGO composites with varying LDH-to-rGO weight ratios (0.25, 0.5, and 0.75). The frequency range spans from 0.1 Hz to 100 kHz [22]. At low frequencies, where interfacial polarization dominates, all samples exhibit increasing impedance with decreasing frequency characteristic of capacitive behavior [21,22]. Among the composites, the **LDH/rGO[0.75]** sample (i.e., high LDH content) demonstrates the highest impedance values, indicating more resistive behavior due to the intrinsically insulating nature of LDH. Conversely, the **LDH/rGO[0.25]** composite (i.e., low LDH and high rGO content) exhibits the lowest impedance across the frequency range, highlighting the significant enhancement in electrical conductivity imparted by the rGO network. The trend clearly shows that increasing the rGO content (decreasing the LDH/rGO ratio) effectively lowers the charge transfer resistance, facilitating faster electron transport. This improvement can be attributed to the superior electrical conductivity of rGO, which serves as an efficient pathway for charge carriers and suppresses the recombination of electrons and holes. The pristine rGO sample, as expected, shows low impedance due to its delocalized π-electron system, while the MgAl-LDH sample presents the highest impedance, consistent with its poor electronic conductivity.

Notably, the **LDH/rGO[0.5]** composite demonstrates intermediate impedance, suggesting a well-balanced structure where the conductive pathways of rGO are maintained while still preserving the functional properties of LDH (e.g., active sites, ion exchange). In summary, the electrochemical impedance results confirm that the integration of rGO into LDH significantly enhances the electrical conductivity of the composites. The LDH/rGO(0.25) composite, with the highest rGO content, emerges as the most conductive material, which is advantageous for applications such as electrocatalysis, sensors, or energy storage systems.

The current–voltage (I–V) response of the synthesized materials MgAl-LDH, rGO, and the LDH/rGO composites with varying ratios (0.25,0.5,0.75) was examined under identical experimental conditions to evaluate their electrocatalytic performance. As depicted in Figure 5c, all samples exhibit typical diode-like behavior with a clear cathodic current increase at negative potentials, indicating efficient charge transfer and catalytic activity. Among all tested materials, the LDH/rGO(0.5) composite displayed the highest current density, suggesting superior charge carrier mobility and enhanced electron transport. This enhancement is attributed to the synergistic effect between the conductive reduced graphene oxide (rGO) and the catalytically active LDH framework. The high surface area of rGO provides efficient pathways for charge transfer, while LDH contributes to catalytic active sites. Notably, the pristine MgAl-LDH and rGO electrodes showed lower current densities compared to the LDH/rGO hybrids, confirming the significance of interfacial contact and electronic coupling in the composites [23]. The improved performance of LDH/rGO(0.5) over LDH/rGO(0.25) and LDH/rGO(0.75) further suggests that an optimal rGO content is essential to balance conductivity and active site availability. These findings are consistent with previous electrochemical impedance spectroscopy (EIS) and Bode plot analyses, reinforcing the conclusion that the LDH/rGO(0.5) composite exhibits superior electrochemical behavior, making it a promising candidate for applications in electrocatalysis and energy conversion devices.

In general, the Mott–Schottky (M–S) analysis is fundamentally based on the formation of a Schottky barrier at the interface between the semiconductor electrode and the electrolyte solution [20]. This interfacial behavior enables the determination of key semiconductor properties,

 doi:10.20944/preprints202510.1526.v1

particularly the carrier density. Therefore, the semiconductor properties of MgAl-LDH, rGO, LDH/rGO(0.25), LDH/rGO(0.5), and LDH/rGO(0.75) were further investigated by M-S plot analysis as shown in Figure 5d. The analysis of MS plots serves as a powerful tool for identifying the type of semiconductor. A positive slope in the M–S plot is indicative of n-type semiconductor behavior, whereas a negative slope corresponds to p-type characteristics, with the direction of inclination relative to the X-axis revealing the dominant charge carrier type. In the present study, the MS plots of the as-prepared electrodes exhibited positive slopes, confirming their n-type semiconductor nature. As shown in Figure 5e, the extrapolated intercept of the linear region of the $1/C^2$ versus potential (E) plot on the potential axis (where $1/C^2 = 0$) represents the flat band potential (V_{fb}). For n-type semiconductors, the flat band potential is approximately equal to the conduction band potential (E_{CB}), while for p-type semiconductors, it approximates the valence band potential (E_{VB}). The flat-band potentials (E_{fb}) of MgAl-LDH, rGO, LDH/rGO(0.25), LDH/rGO(0.5), and LDH/rGO(0.75) were calculated to be −0.38, −0.25, −0.36, −0.34, and −0.33 V vs. Ag/AgCl, respectively. Therefore, the E_{CB} potentials of MgAl-LDH, rGO, LDH/rGO (0.25), LDH/rGO (0.5), and LDH/rGO (0.75) were estimated to be -0.58, -0.45, -0.56, -0.54, and -0.53 V vs. Ag/AgCl, respectively. The cathodic shifting of the E_{fb} of LDH/rGO as compared to rGO and MgAl-LDH strengthened the band bending at the LDH/rGO electrolyte interface, which effectively decreases the carrier recombination close to the Efb. The E_{CB} measured against the Ag/AgCl reference electrode can be converted to the normal hydrogen electrode (NHE) scale using the Nernst equation, as follows:

$$E_{CB}[NHE] = E_{CB}[Ag/AgCl] + E^0_{Ag/AgCl} + 0.059\ pH \quad [20]$$

At 25°C, the standard electrode potential of the Ag/AgCl reference electrode is $E^0_{Ag/AgCl} = 0.197$ V. The conduction band potential obtained experimentally is referenced against this Ag/AgCl electrode. The electrolyte used, 0.5 mol L^{-1} Na_2SO_4, exhibited a measured pH of approximately 6.5. Therefore, the CB potential of MgAl-LDH, rGO, LDH/rGO(0.25), LDH/rGO(0.5), and LDH/rGO(0.75) were estimated to be -0.388, -0.253, -0.36, -0.34, and -0.33 V vs. NHE, respectively. The Scheme 1 study presents a comprehensive analysis of the band edge positions (relative to the Normal Hydrogen Electrode, NHE), bandgap energies, and photocatalytic redox potentials for reduced graphene oxide (rGO), pristine MgAl-layered double hydroxide (LDH), and LDH/rGO composites with varying LDH content (25%, 50%, and 75%). The CB potentials of all samples were found to be more negative than the $O_2/\bullet O_2^-$ potential (−0.33 V vs. NHE), facilitating the generation of superoxide radicals. The VB positions exceeded the oxidation potential threshold for $H_2O/\bullet OH$, thereby enabling hydroxyl radical formation. Notably, as the LDH content increased, the bandgap exhibited a widening trend, ranging from 2.4 to 2.9 eV. The interfacial synergy and photocatalytic efficiency reached a peak at the LDH/rGO (0.5) composite, which demonstrated an optimal balance between active surface sites and charge carrier mobility. The band structures of rGO, MgAl-LDH, and various LDH/rGO composites with different LDH ratios were systematically analyzed to elucidate their photocatalytic behavior.

As illustrated in Scheme 1a, the pristine rGO displayed a narrow bandgap of 2.3 eV; however, its photocatalytic activity was constrained by inadequate oxidative potential and rapid recombination. Conversely, MgAl-LDH exhibited a wider bandgap of 3.5 eV along with favorable redox potentials, yet it was limited by poor visible light absorption. Following the formation of composites, the bandgap of LDH/rGO narrowed in accordance with the LDH content: 2.4 eV for LDH/rGO (0.25), 2.8 eV for LDH/rGO (0.5), and 2.9 eV for LDH/rGO (0.75) in Scheme 1b. All composites-maintained conduction band positions more negative than −0.33 V, thus supporting $\bullet O_2^-$ generation, while their valence bands were sufficiently positive to facilitate •OH formation.

 doi:10.20944/preprints202510.1526.v1

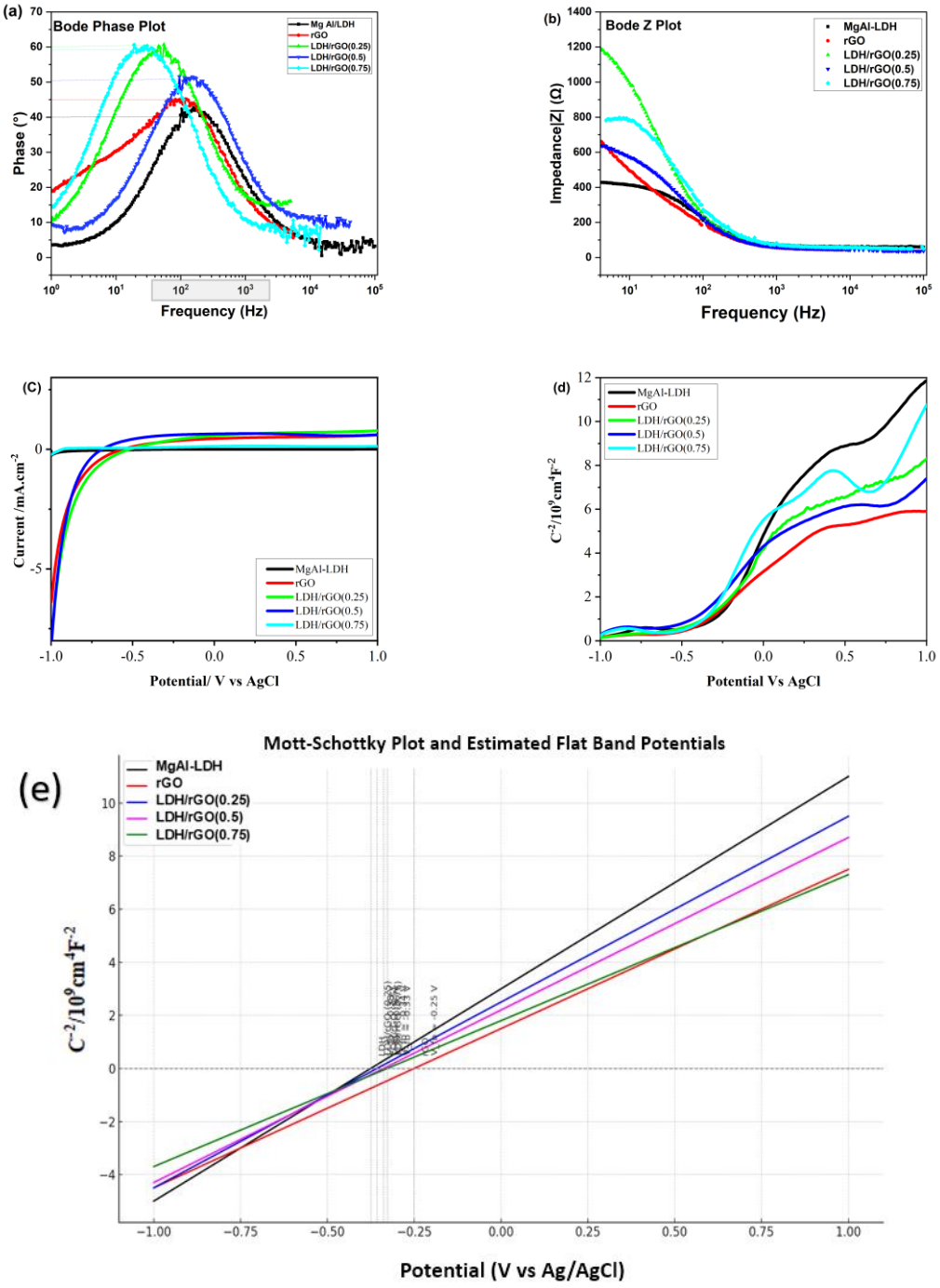

Figure 5. (**a**) Electrochemical impedance spectra (Bode phase plots (**b**) Bode Z plots, (**c**) Photocurrent density plots, and (**d**,**e**) Mott-Schottky plot of MgAl-LDH, rGO, and LDH/rGO (0.25, 0.5, 0.75).

 doi:10.20944/preprints202510.1526.v1

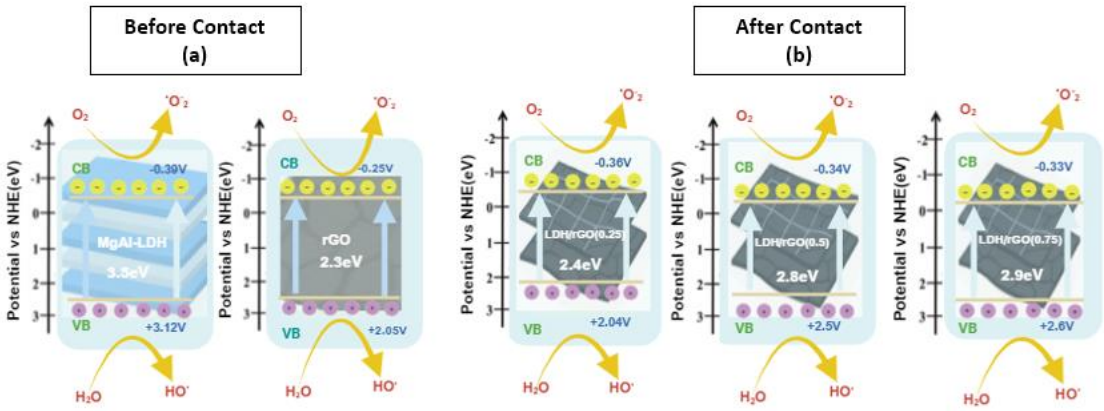

Scheme 1. The representation of band edge alignment and photocatalytic mechanism of modified MgAl-LDH nanocomposites (a): band gap calculated for pure MgAl-LDH before the intercalation with rGO, (b): band gap calculated after intercalation of MgAl-LDH with rGO composites with varying LDH Content (0.25,0.5, &0.75).

2.4. Photocatalytic Activity Assessment

The photocatalytic performance of the synthesized materials was systematically investigated through the degradation of Malachite Green (MG) dye, initially prepared at a concentration of 10 ppm. Experiments were carried out under optimized alkaline conditions (pH = 10) to achieve maximum degradation efficiency. The photocatalysts examined included pristine MgAl–LDH, pure rGO, and a series of rGO-intercalated MgAl–LDH nanocomposites synthesized at different LDH/rGO mass ratios (0.25, 0.5, and 0.75), enabling a comprehensive comparison of their photocatalytic behaviors. The study highlights how the molecular structure and cationic nature of Malachite Green influence its adsorption and subsequent degradation pathway on the catalyst surface, providing deeper insight into the relationship between composite composition and photocatalytic activity.

2.4.1. Influence of dye structure and charge on degradation behavior.

Figure 6 shows the Malachite Green dye, which studied the photocatalytic system, has an extended π-conjugated structure with delocalized π-electrons and is cationic [15,24]. Its degradation activity is to some extent related to the mass ratio of LDH to rGO in the composite. Especially, the degradable efficiency of pure rGO was ~98%, and the LDH/rGO composites also own the high performance when the ratio of LDH/rGO is 0.25 and 0.5 (~93%). However, the efficiency declines drastically at a higher LDH to rGO ratio of 0.75, reaching only ~24%. This behavior can be explained by the strong π–π stacking interactions between the aromatic rings of the target dye (e.g., malachite green) and the graphene sheets, which enhance adsorption onto the rGO surface. Additionally, under alkaline conditions (pH 10), the increased OH^- ion concentration facilitates the generation of hydroxyl radicals (·OH), which are highly reactive and promote effective dye degradation. Nevertheless, a higher proportion of LDH (as in the 0.75 ratio) may lead to reduced photocatalytic activity due to excessive coverage of rGO surfaces, limiting light absorption or promoting particle agglomeration, which in turn suppresses active site accessibility and overall performance. The degradation efficiency (%) can be calculated using the following formula:

$$\boldsymbol{Degradatio\ efficiency}\ (\%) = \left[\frac{\boldsymbol{Initial\ Concentration - Final\ Concentration}}{\boldsymbol{Initial\ Concentration}}\right] * \mathbf{100} \quad [15]$$

2.4.2. Role of pH in Dye Degradation

The role of pH in dye degradation processes is closely related to the nature of the dye itself. This influence stems mainly from three interrelated aspects: the surface charge of the catalyst, which shifts

 doi:10.20944/preprints202510.1526.v1

depending on the pH of the medium; the ionization behavior of the dye molecules; and the ability of the system to generate reactive radicals effectively at different pH levels, as seen in Table 2 for each dye.

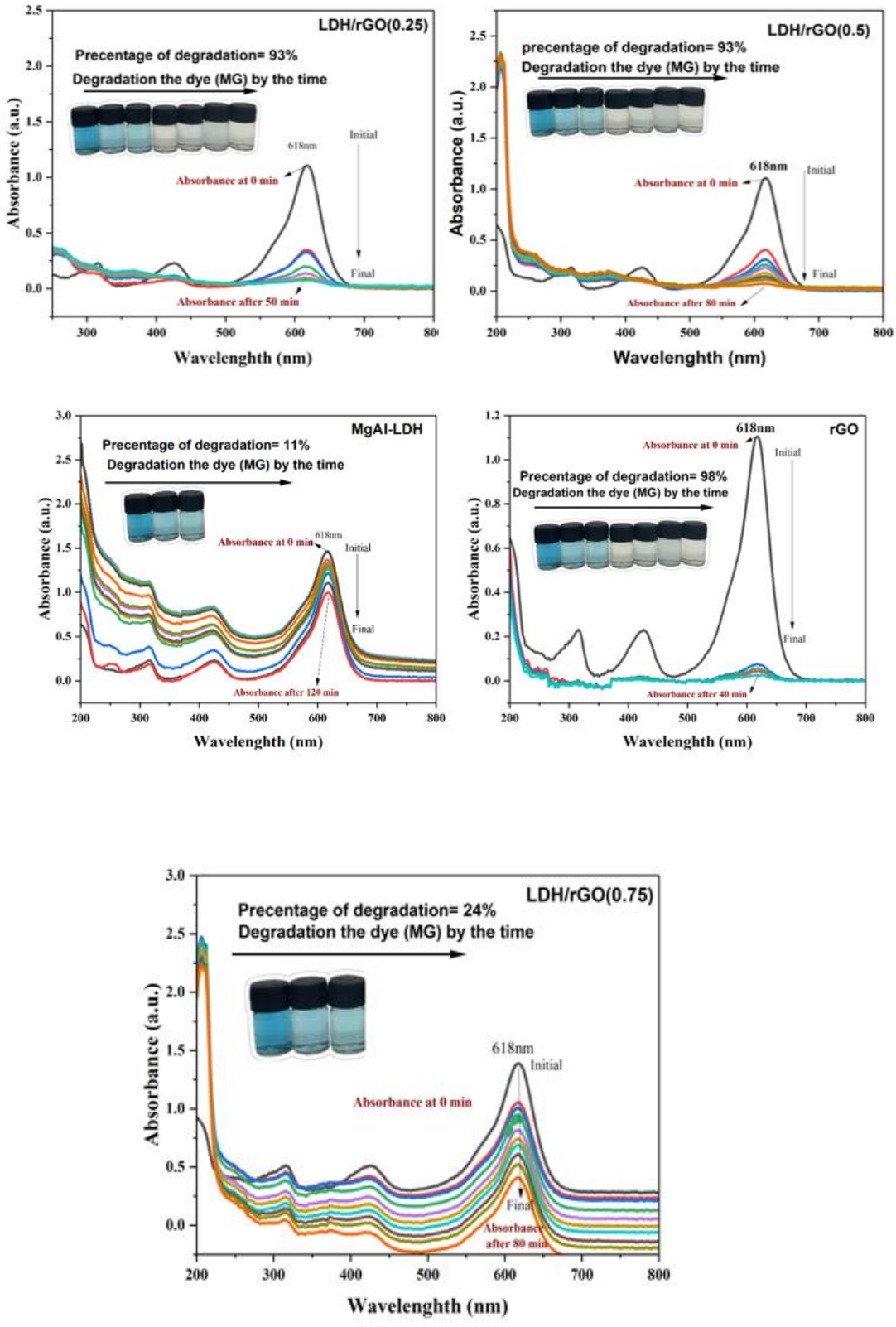

Figure 6. Photocatalytic degradation for MG with varying LDH Content (0.25, 0.5, & 0.75).

Table 2. Comparison of mechanistic effect for the three organic dyes.

 doi:10.20944/preprints202510.1526.v1

Dye	Optimal pH	Mechanistic Effect	Ref
MG	10 (alkaline)	Favors ·OH generation, dye deprotonation, better rGO interaction.	[25]

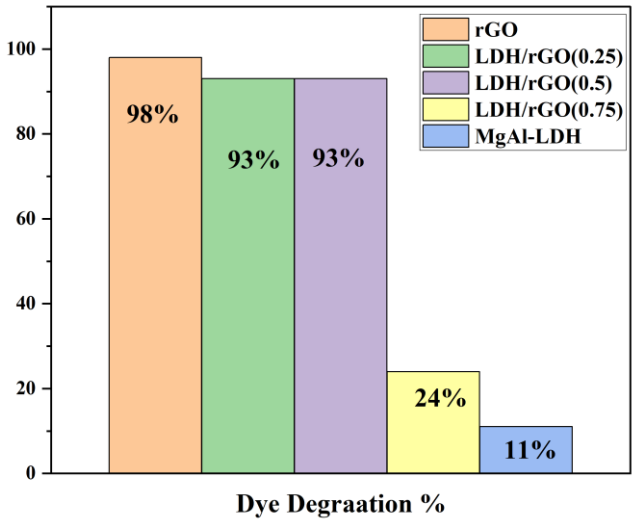

Figure 7. Photocatalytic degradation performance and kinetic behavior of Malachite Green (MG) dye under UV–visible light irradiation using rGO-intercalated MgAl–LDH composites.

2.4.3. Proposed Mechanistic Pathways

The photocatalytic degradation of organic dye such as Malachite Green (MG), using layered double hydroxide/reduced graphene oxide (LDH/rGO) nanocomposites operates via a synergistic mechanism involving light-induced charge separation and the subsequent formation of reactive oxygen species (ROS) [26]. Upon exposure to ultraviolet or visible light, electrons in the valence band (VB) of LDH are excited to the conduction band (CB), leaving behind holes in the VB. The reduced graphene oxide component plays a pivotal role in facilitating efficient charge transfer by acting as an electron acceptor and transporter, thereby suppressing the recombination of electron–hole pairs and prolonging the lifetime of photogenerated charges [27]. These charge carriers trigger a series of surface redox reactions: conduction band electrons reduce dissolved oxygen molecules to generate superoxide radicals ($\bullet O_2^-$), while valence band holes oxidize water or hydroxide ions to produce hydroxyl radicals (•OH). These ROS are the key oxidative species responsible for dye degradation. In the case of malachite green, degradation is initiated by stepwise N-demethylation of the dimethylamino groups, followed by cleavage of the central chromophore structure and aromatic ring opening [28]. This process leads to the formation of smaller intermediate compounds, including carbinolamines and phenolic derivatives, which are subsequently oxidized into low-molecular-weight carboxylic acids. Complete mineralization ultimately yields CO_2, H_2O, and inorganic nitrogen species, as illustrated in Scheme 2.

 doi:10.20944/preprints202510.1526.v1

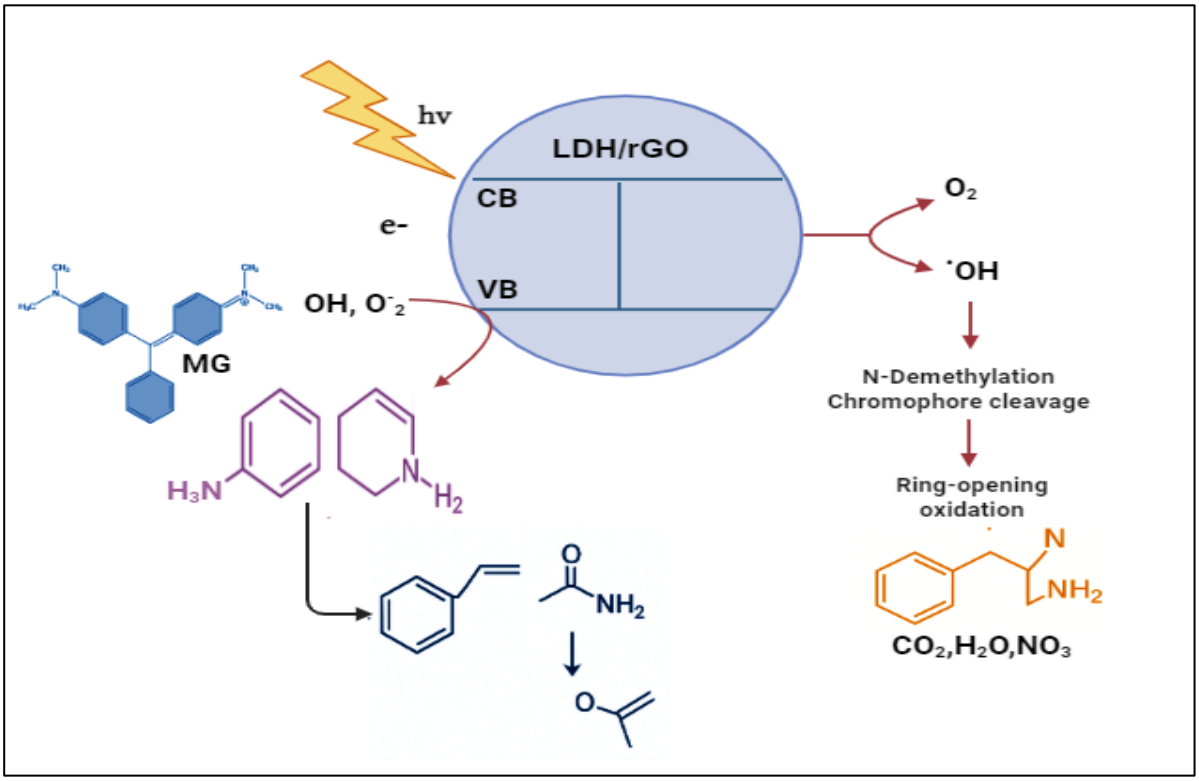

Scheme 2. Mechanism of photodegradation of MG using LDH/rGO nano-catalys.

The photocatalytic degradation of Malachite Green (MG) was found to be the most efficient among all tested systems, reflecting the strong interaction between the dye molecules and the LDH/rGO composite surface. The rGO and LDH/rGO photocatalysts with moderate rGO loadings (0.25 and 0.5) exhibited superior activity compared to pristine LDH, indicating a synergistic effect between the layered double hydroxide matrix and the conductive graphene sheets.

This enhanced performance can be attributed to several factors: (i) improved charge separation and electron mobility facilitated by the rGO network, (ii) increased surface area providing more accessible active sites for dye adsorption, and (iii) favorable electrostatic interaction under alkaline conditions, which promotes the generation of reactive oxygen species (•OH and O_2•$^-$) responsible for dye oxidation.

Overall, the remarkable degradation efficiency of MG under UV–visible illumination confirms that the photocatalytic activity of LDH/rGO composites is strongly dependent on the rGO content and the solution pH. The moderate incorporation of rGO not only enhances light absorption and electron transport but also preserves sufficient hydroxide layers for pollutant interaction, resulting in an optimal balance between adsorption and photodegradation processes.

3. Materials and Methods

3.1. Materials

All chemicals used in this study were of analytical grade and used without further purification. Graphene oxide (GO), magnesium nitrate hexahydrate [$Mg(NO_3)_2{\cdot}6H_2O$, 99%], aluminum nitrate nonahydrate [$Al(NO_3)_3{\cdot}9H_2O$, 98%], potassium hydroxide (KOH, 99%), potassium bicarbonate ($KHCO_3$, 99%), and hexadecyltrimethylammonium bromide (CTAB) were purchased from Sigma-Aldrich (St. Louis, MO, USA). Hydrazine hydrate (99%) was obtained from Fluka AG (Buchs, Switzerland). Ammonia solution (NH_3) and absolute ethanol were procured from BDH (Poole, UK).

3.2. Synthesis of Mg–Al LDH and LDH/rGO Nanocomposites via Ultrasonic-Assisted Co-Precipitation and CTAB-Templated Hydrothermal Methods.

 doi:10.20944/preprints202510.1526.v1

MgAl-layered double hydroxide (LDH) samples with a molar Mg/Al ratio of 3:1 was synthesized via a conventional co-precipitation method under ultrasonic irradiation. Aqueous solution A was prepared by dissolving stoichiometric amounts of magnesium nitrate and aluminum nitrate in deionized water. Solution B consisted of a mixture of 1 M KOH and 0.5 M $KHCO_3$, which was allowed to equilibrate for 72 h. The detailed synthesis procedures, including reaction conditions and schematic representations (S1-S3).

3.3. Characterization Techniques

A range of characterization techniques was employed to analyze the synthesized bare and LDH/rGO samples, as detailed in the supplementary materials.

3.4. Photocatalytic Study

The photocatalytic degradation performance of MgAl-Layered Double Hydroxide and its composites with reduced graphene oxide (LDH/rGO) was evaluated against various organic dyes, including Malachite Green (MG). The experimental procedure was divided into three main steps:

Step 1: Sample Preparation

Aqueous dye solution (20 mL) was prepared with an initial concentration of 10 ppm. Optimization degradation includes variations in pH at a range (1, 3, 5, 7, and 10). Three composite catalysts with varying LDH/rGO weight ratios (0.25, 0.5, and 0.75) were utilized to examine the influence of rGO content on photocatalytic efficiency. For each reaction, 5 mg of catalyst was added to the dye solution.

Step 2: Adsorption–Desorption Equilibrium (Dark Reaction)

Prior to light irradiation, the dye-catalyst suspensions were stirred in the dark for 30 minutes to establish adsorption-desorption equilibrium between the dye molecules and the catalyst surface. This step ensures that any subsequent dye removal is due to photocatalytic activity rather than simple adsorption.

Step 3: Photocatalytic Reaction under Visible Light

The suspensions were then exposed to visible light to initiate the photocatalytic degradation. At specific time intervals, aliquots were withdrawn and centrifuged to remove the catalyst. 10, 20, 30, 40, 50, 60, 70, 80, 90, 100, 110, and 120 minutes. Degradation is carried out using UV light. The supernatants were analyzed using a UV-Vis spectrophotometer to monitor the degradation of dye molecules by measuring the decrease in absorbance at the dye's characteristic wavelength at Figure 8.

 doi:10.20944/preprints202510.1526.v1

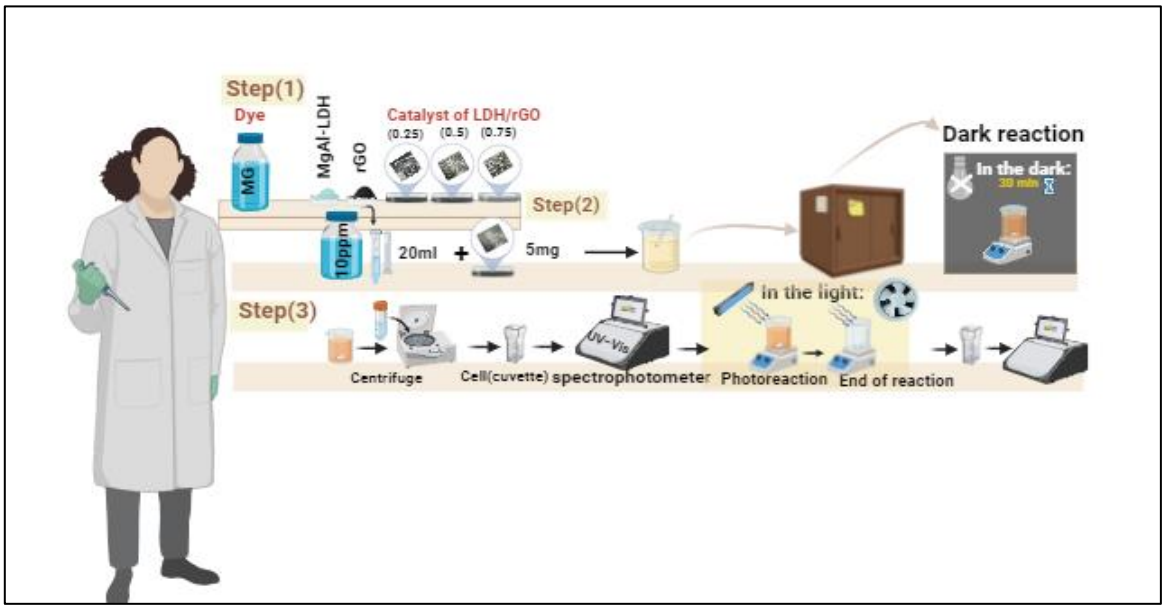

Figure 8. Experimental workflow of photocatalytic dye degradation using LDH/rGO composites under UV-visible light.

4. Conclusions

In this study, MgAl–LDH intercalated with reduced graphene oxide (rGO) was successfully synthesized and systematically characterized to evaluate its structural, surface, and photocatalytic properties toward the degradation of Malachite Green (MG) under UV–visible illumination. The integration of rGO within the LDH matrix profoundly enhanced the physicochemical performance of the composite by improving electrical conductivity, increasing surface area, and facilitating efficient charge separation between photoinduced electrons and holes.

Among the prepared series, the LDH/rGO composites containing moderate rGO ratios (0.25–0.5) exhibited superior photocatalytic activity, demonstrating the critical role of interfacial synergy between LDH layers and graphene domains. This balanced composition effectively combined high surface reactivity with optimal light-harvesting ability, leading to rapid MG degradation under alkaline conditions. The process followed a pseudo-first-order kinetic behavior, highlighting the dominant influence of surface adsorption and reactive oxygen species generation (•OH and O_2•$^-$) in the overall degradation mechanism.

The findings confirm that rGO not only acts as an electron mediator but also contributes to enhancing active site accessibility and dye adsorption, resulting in an integrated adsorption–photocatalysis mechanism. This work provides valuable insight into the design of hybrid LDH–carbon nanostructures with tailored interfaces for sustainable water purification applications. Future investigations may focus on extending this approach to other organic contaminants, exploring visible-light-driven modifications, and assessing catalyst stability under continuous irradiation for practical environmental deployment.

Supplementary Materials: The following supporting information can be downloaded at the website of this paper posted on Preprints.org.

Author Contributions: Original draft preparation, H.T.A., and G.A.; Writing—review and editing M.M.M.M.; Supervision, M.M.M.M. All authors have read and agreed to the published version of the manuscript.

Funding: This research was funded by the Deanship of Scientific Research at King Abdulaziz University under Grant No. (IPP 299-130-2025).

Data Availability Statement: Not applicable here.

Acknowledgments: Acknowledgments: This project was funded by Deanship of Scientific Research (DSR) at King Abdulaziz University, Jeddah, under grant no.IPP 299-130-2025. The authors, therefore, acknowledge with thanks DSR for technical and financial support.

Conflicts of Interest: The authors disclosed no conflicts of interest.

References

1. Ahmad N, Savira D, Erviana D, Mohadi R, Lesbani A. A series of MgAl layer double hydroxide-based materials intercalated with Clitoria ternatea flower extract as photocatalysts in the ciprofloxacin degradation. Chem Phys Impact. 2024;8:100587.
2. Al-Nuaim MA, Alwasiti AA, Shnain ZY. The photocatalytic process in the treatment of polluted water. Chem Pap. 2023 Feb 1;77(2):677–701.
3. Gu Y, Yang Z, Zhou J, Fang Q, Tan X, Long Q. Graphene/LDHs hybrid composites synthesis and application in environmental protection. Sep Purif Technol. 2024 Jan 1;328:125042.
4. Gu Y, Yang Z, Zhou J, Chen Z. Application of graphene/LDH in energy storage and conversion. Sustain Mater Technol. 2023 Sept 1;37:e00695.
5. Raghuwanshi M, Singh A, Suryawanshi B, Jaiswal Y. Synthesis and characterization of MgAl- layered double hydroxide with graphene oxide intercalation: Application in lead removal from spent batteries effluent. Mater Today Proc. 2024 Jan 1;111:121–8.
6. Chaudhuri H, Yun YS. Synthesis and environmental applications of graphene oxide/layered double hydroxides and graphene oxide/MXenes: A critical review. Sep Purif Technol. 2022 Sept 15;297:121518.
7. Cao Y, Li G, Li X. Graphene/layered double hydroxide nanocomposite: Properties, synthesis, and applications. Chem Eng J. 2016 May 15;292:207–23.
8. Chen CC, Lu CS. Mechanistic Studies of the Photocatalytic Degradation of Methyl Green: An Investigation of Products of the Decomposition Processes. Environ Sci Technol. 2007 June 1;41(12):4389–96.
9. Khan S, Noor T, Iqbal N, Yaqoob L. Photocatalytic Dye Degradation from Textile Wastewater: A Review. ACS Omega. 2024 May 21;9(20):21751–67.
10. Visible Light-Driven Photocatalytic Degradation of Methylene Blue Dye Using a Highly Efficient Mg–Al LDH@g-C3N4@Ag3PO4 Nanocomposite | ACS Omega [Internet]. [cited 2025 July 14]. Available from: https://pubs.acs.org/doi/full/10.1021/acsomega.3c07326
11. Djeda R, Mailhot G, Prevot V. Porous Layered Double Hydroxide/TiO2 Photocatalysts for the Photocatalytic Degradation of Orange II. ChemEngineering. 2020 June;4(2):39.
12. Laipan M, Yu J, Zhu R, Zhu J, Smith AT, He H, et al. Functionalized layered double hydroxides for innovative applications. Mater Horiz. 2020 Mar 9;7(3):715–45.
13. Manuda KRJ, Tillekaratne A, Jayasundara DR. In situ real-time assessment of wavelength dependent degradation of methyl orange on rGO-TiO2 photocatalyst. iScience. 2025 May;28(5):112304.
14. Farhan A, Khalid A, Maqsood N, Iftekhar S, Sharif HMA, Qi F, et al. Progress in layered double hydroxides (LDHs): Synthesis and application in adsorption, catalysis and photoreduction. Sci Total Environ. 2024 Feb 20;912:169160.
15. Hanifah Y, Mohadi R, Mardiyanto M, Lesbani A. Photocatalytic Degradation of Malachite Green by NiAl-LDH Intercalated Polyoxometalate Compound. Bull Chem React Eng Catal. 2022 Sept 30;17(3):627–37.
16. Rajoba SJ, Sartale SD, Jadhav LD. Investigating functional groups in GO and r-GO through spectroscopic tools and effect on optical properties. Optik. 2018 Dec;175:312–8.
17. Li B, Zhao Y, Zhang S, Gao W, Wei M. Visible-Light-Responsive Photocatalysts toward Water Oxidation Based on NiTi-Layered Double Hydroxide/Reduced Graphene Oxide Composite Materials. ACS Appl Mater Interfaces. 2013 Oct 23;5(20):10233–9.
18. Nayak S, Parida K. Recent Progress in LDH@Graphene and Analogous Heterostructures for Highly Active and Stable Photocatalytic and Photoelectrochemical Water Splitting. Chem – Asian J. 2021;16(16):2211–48.
19. Ma X, Liu T, Liu E, Zhang Y. Preparation and performance of Cd-MgAl-LDHs@RGO in high efficiency electrocatalytic reduction of CO2 to CO. Mol Catal. 2023 Jan 15;535:112876.

 doi:10.20944/preprints202510.1526.v1

20. Nayak S, Parida KM. Deciphering Z-scheme Charge Transfer Dynamics in Heterostructure NiFe-LDH/N-rGO/g-C3N4 Nanocomposite for Photocatalytic Pollutant Removal and Water Splitting Reactions. Sci Rep [Internet]. 2019 Feb 21 [cited 2025 July 8];9(1). Available from: https://www.nature.com/articles/s41598-019-39009-4
21. Zhang L. Photocatalysts with adsorption property for dye-contaminated water purification [Internet] [PhD Thesis]. The University of Queensland; 2017 [cited 2025 July 8]. Available from: http://espace.library.uq.edu.au/view/UQ:656461
22. Mureseanu M, Cioatera N, Carja G. Fe-Ce/Layered Double Hydroxide Heterostructures and Their Derived Oxides: Electrochemical Characterization and Light-Driven Catalysis for the Degradation of Phenol from Water. Nanomaterials. 2023 Jan;13(6):981.
23. Wang HW, Bringans C, Hickey AJR, Windsor JA, Kilmartin PA, Phillips ARJ. Cyclic Voltammetry in Biological Samples: A Systematic Review of Methods and Techniques Applicable to Clinical Settings. Signals. 2021 Mar;2(1):138–58.
24. Amara UE, Majeed A, Al-Rawi SS, Iqbal MA, Shahzadi A, Zakaria M, et al. Harnessing Nanotechnology for Sunlight-Driven Detoxification: Advanced Photocatalytic Strategies for Malachite Green Degradation. Comments Inorg Chem. 2025 May 31;1–45.
25. Yadav P, Manori S, Shukla RK. Contact electro catalysis driven degradation of malachite green dye by RGO/ZnO nanohybrid. Solid State Commun. 2024 Oct 1;389:115578.
26. Hanifah Y, Mohadi R, Mardiyanto, Lesbani A. Polyoxometalate Intercalated MgAl-Layered Double Hydroxide for Degradation of Malachite Green. Ecol Eng Environ Technol [Internet]. 2023 [cited 2025 Oct 12];Vol. 24, iss. 2. Available from: http://yadda.icm.edu.pl/baztech/element/bwmeta1.element.baztech-1e8ce9dc-3303-4e27-a6fe-29b8070cbc56
27. Pattanaik R, Pradhan D, Kamal R, Dash SK. Facile synthesis of Sr-Bi4Ti3O12: A promising photocatalyst for enhanced degradation of malachite green dye under solar irradiation. Mater. 2025 July 1;8:100847.
28. Balderas-León I, Silva-Jara JM, López-Álvarez MÁ, Ortega-Gudiño P, Barrera-Rodríguez A, Neri-Cortés C. Degradation of Malachite Green Dye by Solar Irradiation Assisted by TiO2 Biogenic Nanoparticles Using Vaccinium corymbosum Extract. Sustainability. 2024 Jan;16(17):7638.